Available online at www.sciencedirect.com
ScienceDirect
Remote Sensing of Environment 109 (2007) 81–94
Remote Sensing of Environment
www.elsevier.com/locate/rse

Comparison and validation of MODIS and VEGETATION global LAI products over four BigFoot sites in North America

Jan Pisek *, Jing M. Chen

Department of Geography and Program in Planning, University of Toronto, 100 St. George Street, Room 5047, Toronto, Ontario, Canada M5S 3G3

Received 28 August 2006; received in revised form 8 December 2006; accepted 9 December 2006

Abstract

A new set of recently developed leaf area index (LAI) algorithms has been employed for producing a global LAI dataset at 1 km resolution and in time-steps of 10 days, using data from the Satellite pour l'observation de la terre (SPOT) VEGETATION (VGT) sensor. In this paper, this new LAI product is compared with the global MODIS Collection 4 LAI product over four validation sites in North America. The accuracy of both LAI products is assessed against seven high resolution ETM+ LAI maps derived from field measurements in 2000, 2001, and 2003. Both products were closely matched outside growing season. The MODIS product tended to be more variable than the VGT product during the summer period when the LAI was maximum. VGT and ETM+ LAI maps agreed well at three out of the four sites. The median relative absolute error of the VGT LAI product varied from 24% to 75% at 1 km scale and it ranged from 34% to 88% for the MODIS LAI product. The importance of correcting field measurements for the clumping effect is illustrated at the deciduous broadleaf forest site (HARV). Inclusion of the sub-pixel land cover information improved the quality of LAI estimates for the prairie grassland KONZ site. Further improvement of the global VGT LAI product is suggested by production and inclusion of pixel-specific global foliage clumping index and forest background reflectance maps that would serve as an input into the VGT LAI algorithms.

Keywords: VEGETATION; MODIS; ETM+; BigFoot; LAI; Validation

1. Introduction

Exchanges of energy (Bonan, 1995; Sellers et al., 1994), water (Band et al., 1991; Nouvellon et al., 2000; Su, 2000) and greenhouse gases (Coops et al., 2001; Frank, 2002; Liu et al., 1997; Nouvellon et al., 2000) between the land surface and the atmosphere depend greatly on the functioning of plant leaves. Models that simulate these exchanges require quantitative information on the area and density of vegetation (Dickinson, 1995). Leaf Area Index (LAI) is a key quantitative information in this context (Buermann et al., 2002), where LAI is defined as one half of the total green leaf area per unit ground surface area (Chen & Black, 1992).

For effective use in ecosystem models for large area applications, LAI data must be collected for a long period of time and should represent every region of the terrestrial surface (Myneni et al., 2002). Also, due to different definitions of LAI, different measurement protocols and instruments and different considerations of canopy architecture, LAI products can vary significantly, and it is desirable to have accurate and consistent products for global and regional applications (Deng et al., 2006). Satellite remote sensing is the most effective means of collecting such global fields on a regular basis. Global LAI estimates have been routinely produced using MOderate Resolution Imaging Spectroradiometer (MODIS) data at 1 km resolution and time-intervals of 8 days (Myneni et al., 2002). In the MODIS algorithm, a three-dimensional canopy radiative transfer model is used to derive relationships between the spectral signatures of a vegetated canopy and its structural characteristics (Knyazikhin et al., 1998a,b; Myneni et al., 1997). These relationships are used to relate LAI to measured spectral reflectances at various observation angles. Various levels of accuracy and success have been reported in MODIS product evaluation studies (Abuelgasim et al., 2006; Cohen et al., 2006a, 2003; Fensholt et al., 2004; Huemmrich et al., 2005; Tan et al., 2005; Wang et al., 2004).

* Corresponding author. Tel.:+1 416 978 5070.
E-mail address: jan.pisek@utoronto.ca (J. Pisek).

0034-4257/$ - see front matter © 2007 Elsevier Inc. All rights reserved.
doi:10.1016/j.rse.2006.12.004

Based on previous works (Brown et al., 2000; Chen, 1996; Chen & Cihlar, 1997; Chen & Leblanc, 1997, 2001; Chen et al., 2002; Roujean et al., 1992), Deng et al. (2006) developed a new set of LAI algorithms for the purpose of deriving an alternative global LAI product, using SPOT-4 VEGETATION (VGT) data. The initial validation of this new product included seven sites in Canada (Pisek et al., in press). A limited mutual comparison of MODIS and VGT LAI products was also carried out. However, there was an obvious need for further validation outside of Canada to demonstrate the reliability of this global product. In this study, we carry out comparisons of MODIS and VGT LAI products over a set of LAI reference sites.

One set of LAI data that is optimal for this study is the BigFoot (http://www.fsl.orst.edu/larse/bigfoot/) (Running et al., 1999). The BigFoot project covers nine flux tower sites from Alaska to Brazil represent different biomes. Field data were collected over 25 km^2, and Landsat-7 Enhanced Thematic Mapper Plus (ETM+) image data and ecosystem process models were used to characterize an area of 7 km × 7 km around each tower (Cohen et al., 2006a, 2003). Since the BigFoot LAI ETM+ maps are estimated by independent measurements from both MODIS and VGT products, direct comparisons of BigFoot data with MODIS- and VGT-derived products can help us to assess the quality of these products and the sources of their errors. The validation procedures are in agreement with the outlines presented in Morisette et al. (2006). At most BigFoot sites, there is an existing program of long-term measurements offering LAI data from various years within the growing season. The use of this dataset can thus offer insights into the inter-annual and seasonal variations of LAI.

The aim of this paper is to conduct MODIS and VGT LAI product validation to assess their quality. Four sites with multiple year data from the BigFoot project are selected for this validation. The mutual comparisons of these two products are also made over the seasonal cycles at the four sites in 2000, 2001, and 2003.

2. Materials

2.1. Study sites

The four BigFoot sites included in this study are AGRO (an agricultural system in Bondville, Illinois, USA), HARV (Harvard Forest, Massachusetts, USA), KONZ (Konza Prairie, Kansas, USA), and NOBS (Northern Old Black Spruce, Manitoba, Canada). Campbell et al. (1999) provide detailed descriptions of these sites. The AGRO site is centered at 40.01° N and 88.29° W. The land cover consists of fields with annually harvested crops (Cohen et al., 2003) and a rural community occupying the southeastern corner of the site. The Harvard forest site (HARV; 42.37° N, 72.25° W) represents a temperate mixed forest (Magill et al., 2004). In addition to the closed forest canopies there are a few areas of wetlands, grasslands and water bodies. KONZ (39.08° N, 96.62° W) is predominantly a tallgrass prairie. In the northern part of the site there are areas of deciduous broadleaf forest (Hall et al., 1990). The NOBS site (55.88° N, 98.48° W) has a cover of up to 70% of black spruce forest, comprised of mature stands of trees from 60–120 years in age with tree heights ranging from 7–18 m (Kimball et al., 1997). This site was previously used in the Boreal Ecosystem Atmosphere Study (BOREAS, Sellers et al., 1997). A fire damaged the extreme southern part of the study site in 1981, but the forest has largely recovered since then.

2.2. ETM+ imagery

Table 1 presents a list of seven ETM+ LAI scenes (UTM projection, pixel resolution of 25 m) that were acquired from the BigFoot database (Cohen et al., 2006b). Two scenes were obtained for each site — one map in 2000 and the other in 2001. There was only one scene available from the AGRO site in 2000. Since the site is predominantly occupied by annually harvested crops and no significant differences were expected between the various years in the seasonal LAI cycle, the identical scene was used for the approximate validation of the VGT product performance during 2001 as well. For each scene, the IGBP land cover information has also been acquired (Cohen et al., 2006a). AGRO land cover classification included BigFoot labels (for the IGBP cropland label, it is specified as soybean or corn).

ETM+ LAI estimates are directly linked to the field measurements using methods described by Gower et al. (1999). Cohen et al. (2003) discusses the conversion of the ETM+ spectral data to Tasselled Cap indices. The indices were subsequently related to the field LAI measurements by means of Ordinary Least Squares (OLS) and Reduced Major Axis (RMA) regressions. Cohen et al. (2003) also provide details on the LAI prediction accuracy. It is important to note that during field measurements not all land cover types were sampled (e.g. deciduous broadleaf forest at the KONZ site), and Cohen et al. (2003) used LAI values from literature for these cover types.

2.3. VGT LAI product

Based on a geometrical optical model (Four Scale; Chen & Leblanc, 1997) with a multiple scattering scheme (Chen & Leblanc, 2001) and LAI algorithms previously derived for Canada-wide applications, Deng et al. (2006) produced a new algorithm for the global retrieval of LAI. The algorithm makes use of red, near infrared, and shortwave infrared bands from a satellite sensor. Global scenes of VGT data are acquired over a large ranges of solar zenith and satellite view angles, and a bidirectional reflectance distribution function (BRDF) is needed for correcting these angular effects and standardization of the collected data

Table 1
Dates of BigFoot maps used for validation

Site	Date
AGRO	11-Aug-2000
HARV	4-Aug-2000
	26–28-Jul-2001
KONZ	6-Jun-2000
	18-Jun-2001
NOBS	14-Jul-2000
	14-Jul-2001

(Schaaf et al., 2002). While the usual approach is to conduct BRDF normalization prior to the input of reflectance values into LAI algorithms (Chen, 1996; Chen et al., 2002), BRDF is considered explicitly in the algorithm here. The issue is solved by using the Four Scale model for simulating the relationships between LAI and the spectral bands. Since the vegetation structure is distinctly different among land cover types, the simulations are made separately for different plant functional types. The global land cover classification for the year 2000 (GLC2000) dataset (Bartholomé & Belward, 2005; Loveland et al., 2000) has been used for retrieving the land cover information. The cover types with similar structural characteristics were combined to form six groups based on canopy architecture. The six biomes are (i) needleleaf forest, (ii) tropical forest, (iii) broadleaf forest, (iv) mixed forest, (v) shrub, (vi) cropland and grassland. Snow/ice, water body classes, and bare rock were assigned the value of zero in LAI retrieval.

Based on the model simulations, Deng et al. (2006) fit the key coefficients in the BRDF kernels with Chebyshev polynomials of the second kind. The spectral bands are combined into Simple Ratio (SR) and the Reduced Simple Ratio (RSR) for LAI retrieval. More detail of the theoretical basis of the algorithms is given in Deng et al. (2006).

Since VGT is a single-view angle sensor at each ground location per overpass, the reflectances are mostly affected by the canopy gap fraction at the view angle (Chen, 1996; Harding et al., 2001; Weiss et al., 2000). An assumption of the random leaf spatial distribution is made to invert from gap fraction to LAI. Under this assumption, the inverted LAI is termed the "effective LAI" rather than the true LAI (Chen et al., 1997). It is necessary to convert the effective LAI using the clumping index to retrieve true LAI values. Chen et al. (2005) recently undertook the first ever global mapping of the vegetation clumping index using POLDER measurements. Using their results, mean values for different land cover types were retrieved and used as inputs into the LAI algorithms. It was not possible to include the specific value for clumping index for every pixel on a given date because only eight months of global POLDER-1 at 7 km resolution were available (Lacaze et al., 2002).

The VGT data used in this study were acquired in the form of 10-day composite (S10) scenes from the SPOTIMAGE/VITO distribution site (http://free.vgt.vito.be/). The spatial resolution is 1 km, and the data use the Platee–Carree projection with the WGS84 coordinate system. The annual global VGT LAI product consists of 36 scenes that cover the whole year. We used the data from 2000 and 2001 to match with the maximum number of available ETM+ scenes from the BigFoot project. Since the global VGT LAI product was originally produced for the year 2003, we included these data for the comparison with MODIS LAI as well.

The downloaded VGT data were already atmospherically corrected by the application of the Simplified Method for Atmospheric Correction (SMAC) (Rahman & Dedieu, 1994). However, the residual atmospheric effects were still considerable as abnormally low values within the LAI product were observed, e.g., erratic reductions of LAI up to a value of 6 over 10 days. To minimize these residual atmospheric effects, Chen et al. (2006) developed a procedure named Locally Adjusted Cubic-spline Capping (LACC) to reconstruct the seasonal trajectory of LAI. A series of cubic spline curves are applied to the annual cycle of LAI, and optimum local smoothing coefficients are assigned to every LAI value based on the curvature of the initially fitted curve with an average global smoothing coefficient. In this way, the resulting capping curve is automatically adjusted to both rapid and slow variations in LAI in various seasons. This procedure avoids the problem of rigid seasonal trajectory shapes by simple overlapping of a few harmonics in the existing FASIR (Sellers et al., 1994) and ABC3 (Cihlar et al., 1997) methods. The performance of the LACC method is illustrated in Fig. 1 for one pixel within the AGRO site. The LACC method has been applied to every pixel of the global VGT LAI product.

2.4. MODIS LAI product

The MODIS Collection 4 LAI product and land cover classification schemes were acquired in a form of ASCII subsets from the Distributed Active Archive Center (DAAC) database of Oak Ridge National Laboratory (http://www.modis.ornl.gov/modis/index.cfm). The subset profiles are presented in 1 km resolution with a time-interval of 8 days. The prepared ASCII subsets have already been re-projected and they match the BigFoot sites' layout. The available ASCII subsets were downloaded for the years 2000, 2001, and 2003 to cover the same periods as the VGT LAI product. All mentions of the MODIS product in this paper refer to MODIS Collection 4 unless noted otherwise.

Along with the LAI fields, the Quality Flags for the MODIS product were obtained. Under optimal circumstances, a look-up-table (LUT) method is used to achieve inversion of a three-dimensional radiative transfer model (Myneni et al., 2002). When this method fails to localize a solution, a back-up method based on a relationship between the normalized difference index (NDVI) and LAI (Knyazikhin et al., 1998a; Myneni et al., 1995) is utilized. The Quality Flags serve to determine the origin of the

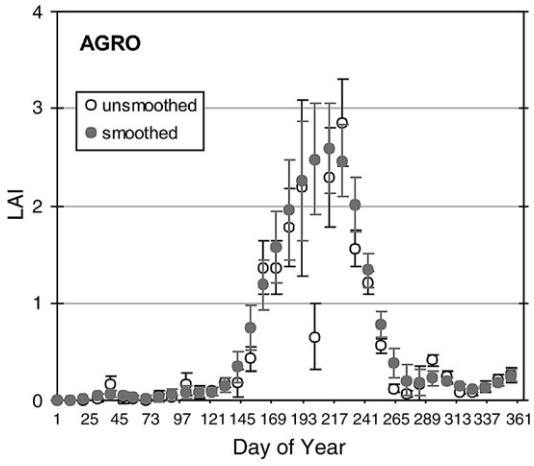

Fig. 1. Comparison of original unsmoothed and temporally smoothed annual LAI cycle at an agricultural system at AGRO site near Bondville, IL for year 2003.

Table 2
List of IGBP land cover classes, present at BigFoot sites, and their codes as used in Fig. 1

IGBP class code	Land cover type
1	Needleleaf evergreen forest
4	Deciduous forest
5	Mixed forest
6	Closed shrubland
7	Open shrubland
8	Woody savanna
9	Savanna
10	Grasslands
11	Permanent wetlands
12	Cropland
13	Urban/built-up area
14	Cropland/natural vegetation
16	Barren
0	Water

calculated value or mark pixels where no retrievals were made. Cohen et al. (2003) originally noted the actual descriptions of the Quality Flags in Collection 4 are not easy to understand. The Quality Flags scheme was simplified here to display only whether the value was calculated by the main algorithm, back-up algorithm, or if the value was not retrieved.

3. Methods

The overall quality of LAI products depends on a few key factors that influence the accuracy of the retrievals. The first factor is the uncertainty in the input land cover data. The effect of land cover misclassification for MODIS and VGT products varies depending on the similarity among biomes. MODIS LAI algorithm also employs a six class biome suite defined in Myneni et al. (2002). Myneni et al. (2002) calculated this LAI difference to be up to 50% when distinct biomes are interchanged. We assessed relative proportions of land cover types within every BigFoot site first. This assessment offered an insight into the role of uncertainties in land cover information in actual LAI retrievals that were compared in the next step. Both MODIS and the BigFoot project use IGBP classification, but the share of the land cover classes present might vary due to the different image resolutions (25 m vs. 1 km). GLC2000 land cover types used with the VGT images were transferred into IGBP equivalents.

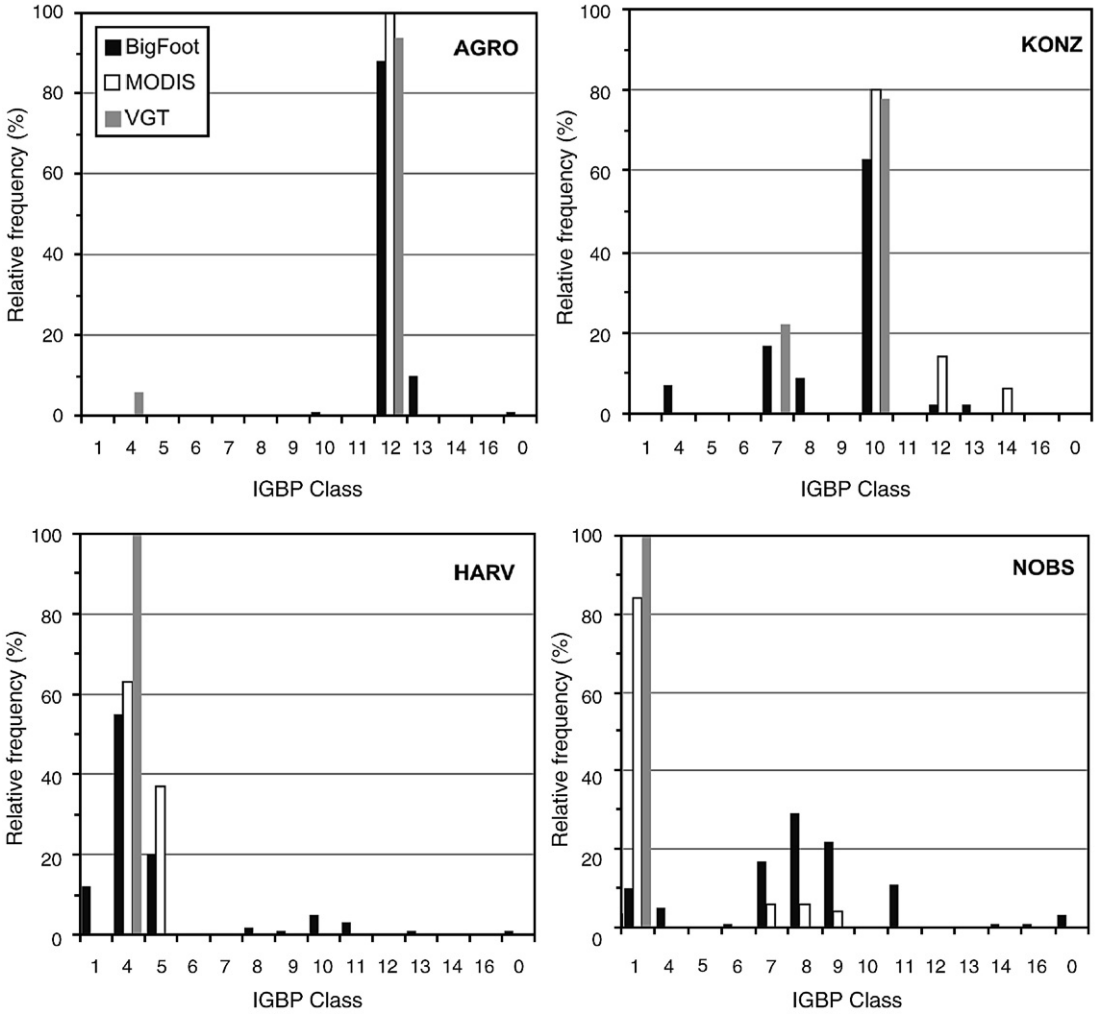

Fig. 2. Relative proportions of land cover types at each site in 2000, as mapped by BigFoot, MODIS, and GLCC 2000. See Table 1 for class names.

Uncertainties and errors in input surface reflectances are another source of possible error in the LAI retrievals (Chen et al., 2002; Fernandes et al., 2003; Yang et al., 2006a). These uncertainties are mainly due to different atmospheric corrections and the length of the composite period. These uncertainties might be larger in the case of the VGT sensor as the composite period is longer than that used for the MODIS sensor. The selected VGT reflectances might come from dates further away from the BigFoot ETM+ maps by a few days. The original reflectance values were available only for the VGT product. Pisek et al. (in press) calculated the mean difference between VGT and Landsat-5 TM vegetation indices to be 14.5% for their set of validation scenes in Canada. We believe the magnitude of the uncertainties introduced by discrepancies in input reflectances between the high resolution and coarse resolution scenes is similar here.

The main step in the validation procedure consisted of placing the BigFoot +ETM LAI data on the graphs containing the MODIS and VGT LAI trajectories for the years 2000, 2001, and 2003. Each data point on the graph has been produced by averaging the LAI values over a 7 km × 7 km BigFoot site. The products are compared over the multi-pixel (patch) rather than on the pixel-by-pixel basis in this step. This strategy reduces errors due to co-registration and overlapping uncertainties between various products (Yang et al., 2006a). Since the LAI values from MODIS can come from the main RT or the back-up algorithm, averages over the BigFoot sites were computed first with main RT retrievals only and then with included back-up values. Tan et al. (2005) advise using back-up algorithm retrievals with caution as they are generated from surface reflectances with high uncertainties. The relative proportion of main and-back up algorithm retrievals has been also assessed to obtain an insight into the seasonal course of plotted MODIS LAI trajectories.

The relatively small size (7 km × 7 km) of the study sites poses limits for testing and comparison of these products via scatter-plots. This is mainly linked to the difficulties of securing the needed close spatial match between the high resolution and low resolution scenes. Also, because of the point spread function behavior of the incoming signal in low resolution sensors, the retrieved value usually comes from a greater area than the actual spatial resolution of the sensor (Cihlar et al.,

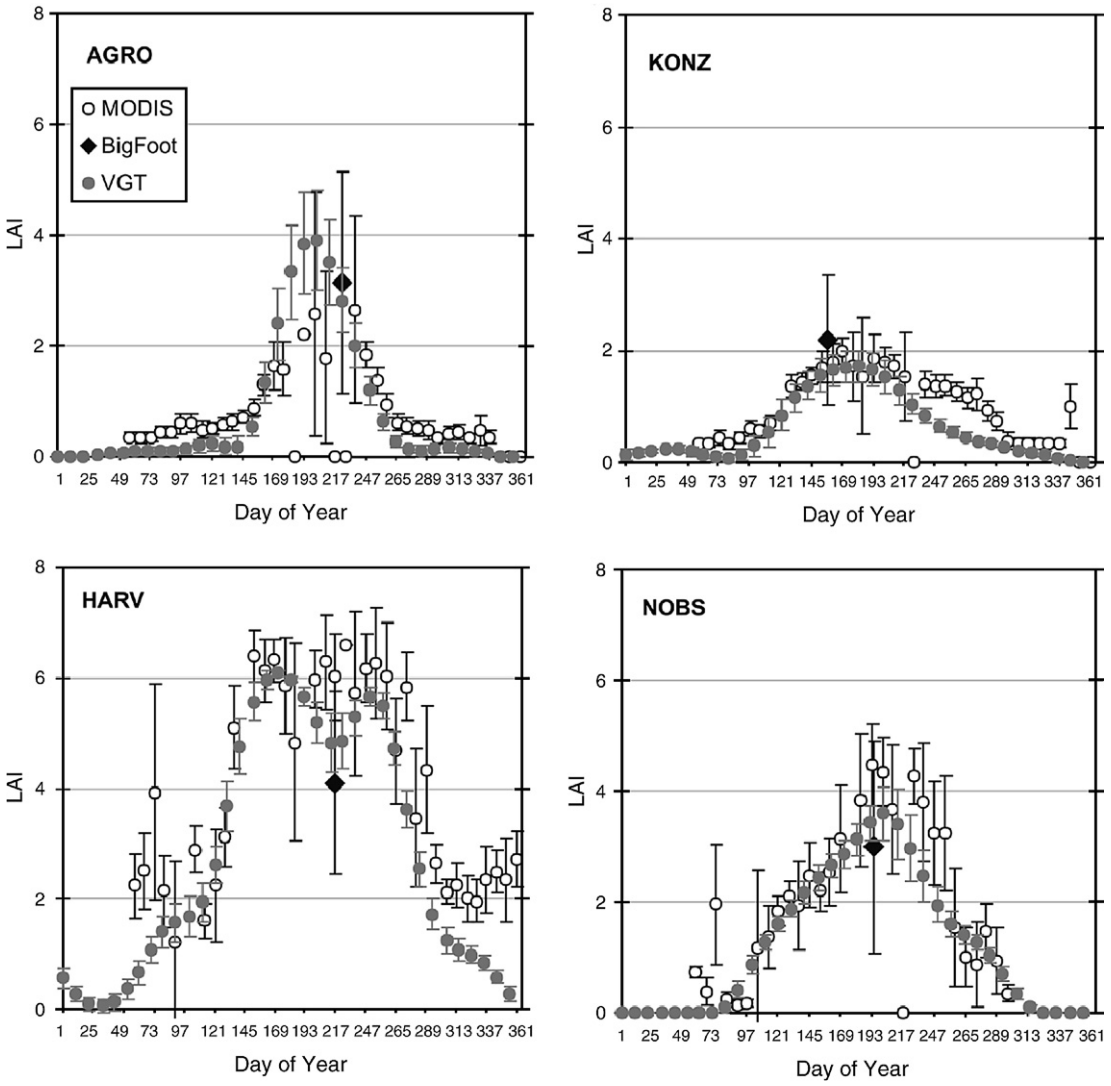

Fig. 3. VGT and MODIS Collection 4 2000 LAI trajectories for each site. Means and one standard deviation values are shown. BigFoot data are shown in black.

Table 3
Summary of LAI statistics of the four ETM+ maps and those of VEGETATION and MODIS over the same scenes in 2000

		AGRO	HARV	KONZ	NOBS
ETM+	Average LAI	3.12	4.10	2.18	2.99
	S.D.	2.00	1.65	1.17	1.92
VGT	Average LAI	2.78	4.81	1.64	3.42
	S.D.	0.67	0.54	0.29	0.32
	RMSE	0.50	1.05	0.79	0.65
MODIS	Average LAI	1.52	6.01	1.78	4.32
	S.D.	0.81	0.79	0.34	0.32
	RMSE	1.61	2.00	0.88	1.90

2003; Cracknell, 1998). Puyou-Lascassies et al. (1994) and Oleson et al. (1995) further demonstrate that the weight of the signal is also not constant over the field of view and decreases with increasing distance from the center. Bearing these limitations in mind, we produced a set of scatter-plots for each BigFoot site. Acquired ASCII subsets of the MODIS product were already pre-processed to fit the 7 km × 7 km sites. Aggregating the values to 1 km resolution produced the equivalent ETM+ LAI estimates. High resolution ETM+ land cover classifications were also used as input into the VGT LAI algorithm. Alternative LAI values for 1-km pixels were then retrieved by weighting the various land cover types by their area fractions within the pixel. The goal of this exercise was to see how the LAI retrievals would change with the inclusion of information about the contexture of low resolution pixels (Chen, 1999) within the validation sites.

4. Results and discussion

4.1. Land cover comparison

Table 2 includes a list of all IGBP classes present at the four sites. The greatest agreement among these classification schemes was observed at the AGRO site (Fig. 2). This was expected, as the AGRO site was quite homogenous in the BigFoot high resolution image with 88% of pixels classified as cropland. The built-up area in the southeastern corner occupied 10% of the total image area. In the MODIS classification all

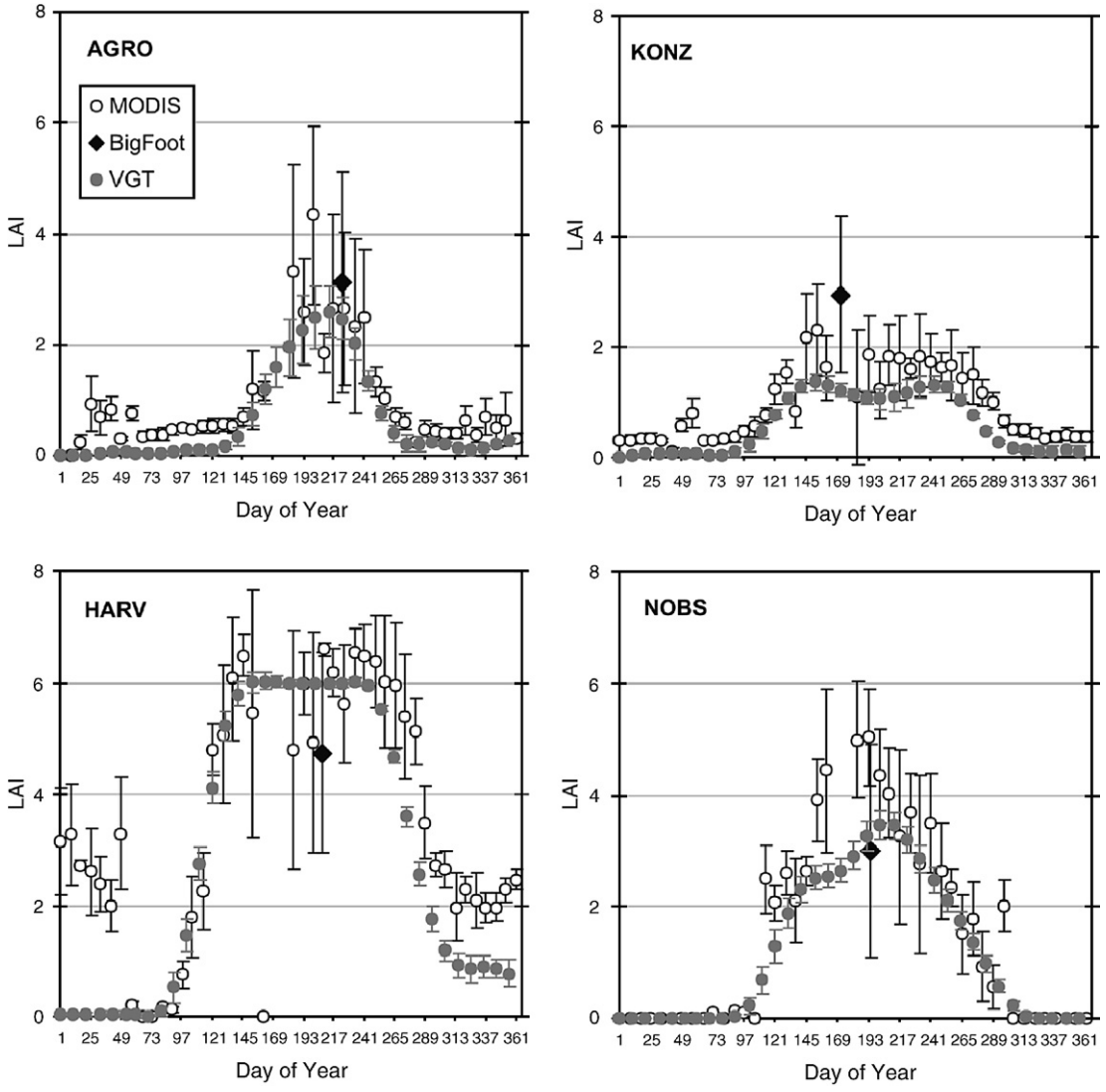

Fig. 4. Same as in Fig. 3, but for year 2001. BigFoot data for AGRO site come from year 2000; for other sites from 2001.

pixels were classified as cropland, and 94% of pixels were identified as cropland in the GLC2000 classification with 6% classified as a deciduous forest. The KONZ site results were also satisfying. Grasslands occupied 78% and 80% in GLC2000 and MODIS classifications, respectively. The share of grassland in the BigFoot image was lower, at 63% with 17% and 9% classified as open shrubland and woody savanna, respectively, and 7% marked as deciduous forest. The differences among the classifications are due to the distributed pattern of deciduous broadleaf forest patches and open shrublands in the BigFoot image, as both low resolution classifications are unable to produce a similar level of detail. The relative share of forest area agrees well in MODIS and BigFoot classifications for the HARV site. MODIS consists of deciduous broadleaf and mixed forest, while BigFoot classifies 12% of pixels as needleleaf evergreen forest. There is a small share of grasslands and permanent wetlands in BigFoot as well. The whole HARV area is classified as broadleaf deciduous forest in GLC2000. Since the RSR-based algorithm is applied for forest pixels in the case of VGT LAI, the land cover discrepancy should not significantly affect the range of retrieved LAI values, as Brown et al. (2000) demonstrated that use of Reduced Simple Ratio (RSR) index reduces the dependence of algorithms on land cover types. The most striking difference in land cover classifications among the low resolution images and BigFoot was observed on the NOBS site. MODIS considers most of the area to be needleleaf evergreen forest whereas BigFoot mapped the site as open shrubland, savanna and woody savanna, and permanent wetland. GLC2000 considered the whole area as a needleleaf evergreen forest. The coniferous forest has been classified as shrubland or woody savanna in the BigFoot project mainly due to the relatively lower density of the forest stands. Random VGT pixels from NOBS site were first marked as a coniferous forest and then as a woody savanna for the LAI algorithm. A difference of LAI > 2 (38%) had been observed for July 21, 2000 — the peak of boreal summer. An additional map source has been consulted for verification of the land cover. It was decided to keep the VGT pixels classified as conifer forest for the next step of constructing the seasonal trajectories of LAI.

4.2. BigFoot–MODIS–VGT comparison: Seasonal trajectories

MODIS LAI estimates were available from February 26, 2000 (day 57) at all sites. Only the MODIS LAI values with the

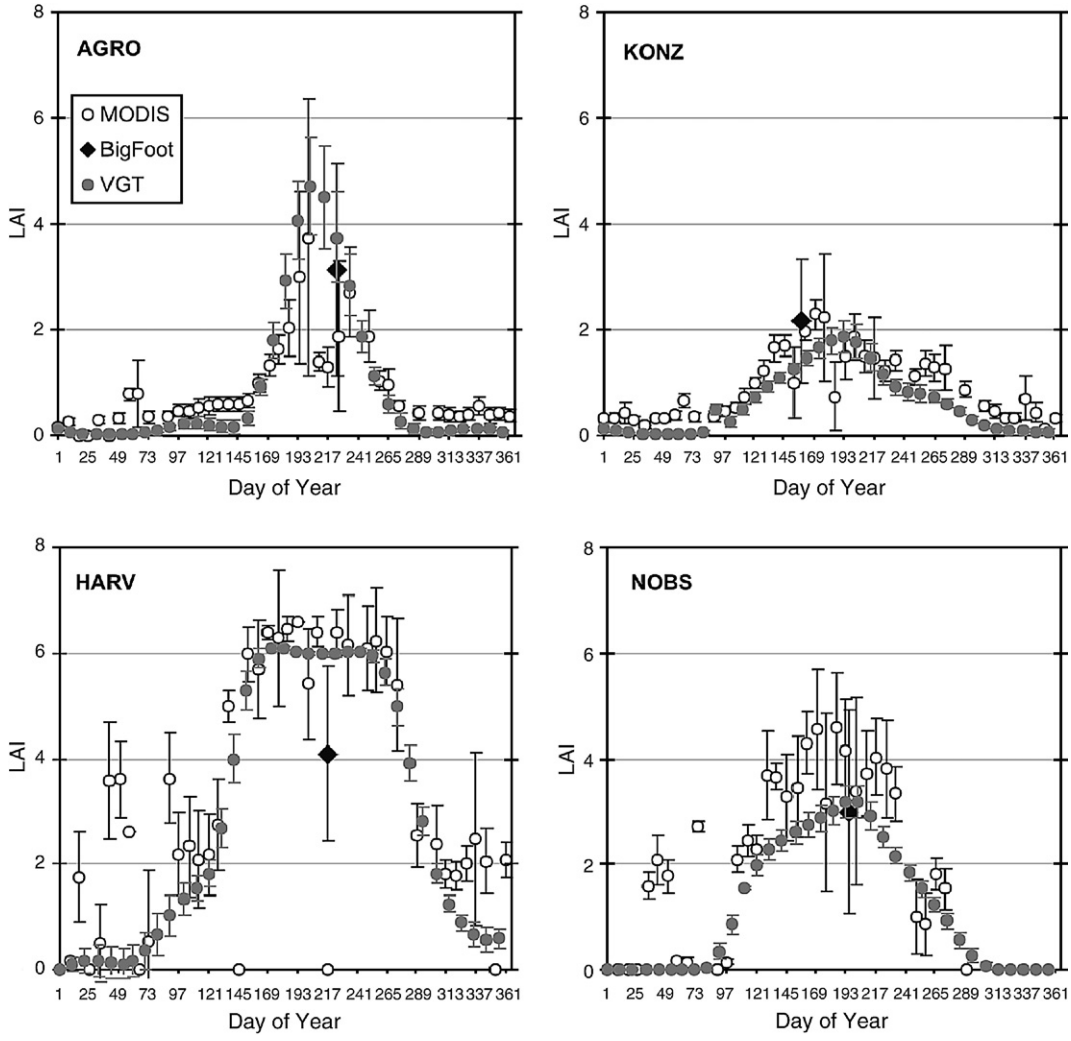

Fig. 5. Same as in Fig. 3, but for year 2003. BigFoot data, shown for comparison, come from year 2000.

highest quality flags were used for the construction of the seasonal trajectories. At the AGRO site, both VGT and MODIS products follow the beginning and the end of the growing season reasonably well, and the differences between the products are minimal (Fig. 3). However, during the peak of the growing season MODIS delivers unstable results. The LACC smoothing method is not used in the MODIS product, although Chen et al. (2006) demonstrated the improvement of the MODIS LAI product if this method is applied. Tan et al. (2005) reported similar unstable behavior for broadleaf and crop pixels for the MODIS Collection 3 product due to mismatch between the modeled and observed MODIS surface reflectances. Yang et al. (2006b) reported that the problem was caused by increased aerosol contamination of surface reflectances. As aerosol contamination increased, the scatter of surface reflectances increased and more data were found to be out of retrieval domain of main RT algorithm. This resulted in the failure of the main algorithm. The BRDF effects are not taken into account within the back-up LAI–NDVI relationships (Shabanov et al., 2005) and the algorithm generates rather unreliable estimates of LAI especially for complicated view geometries. Results from Fig. 3 indicated that the problem persisted in Collection 4 for this agricultural site. The median relative absolute error (RAE) was 88% for the MODIS LAI product, while the RAE of the VGT LAI product was half as low. VGT retrievals after smoothing match the expected seasonal trajectory very well. The maximum LAI value occurs around July 20 (day 202) and it is in good agreement with the seasonal maximum LAI around 4 observed around nearby flux tower sites according to FLUXNET ground measurements (http://www-eosdis.ornl.gov/FLUXNET/). The BigFoot LAI for August 11 also closely agrees with the seasonal trajectory of VGT.

The MODIS and VGT LAI trajectories are in very good agreement up to August 4 at KONZ. MODIS LAI does not decrease below 1 until the beginning of October, while VGT does so two months earlier. At this site, the MODIS LAI estimate is closer to BigFoot than VGT. The difference is still only around LAI of 0.5 between VGT and BigFoot (Table 3).

MODIS estimates for the deciduous HARV site do not decrease below LAI of 2 during the entire year. However, Yang

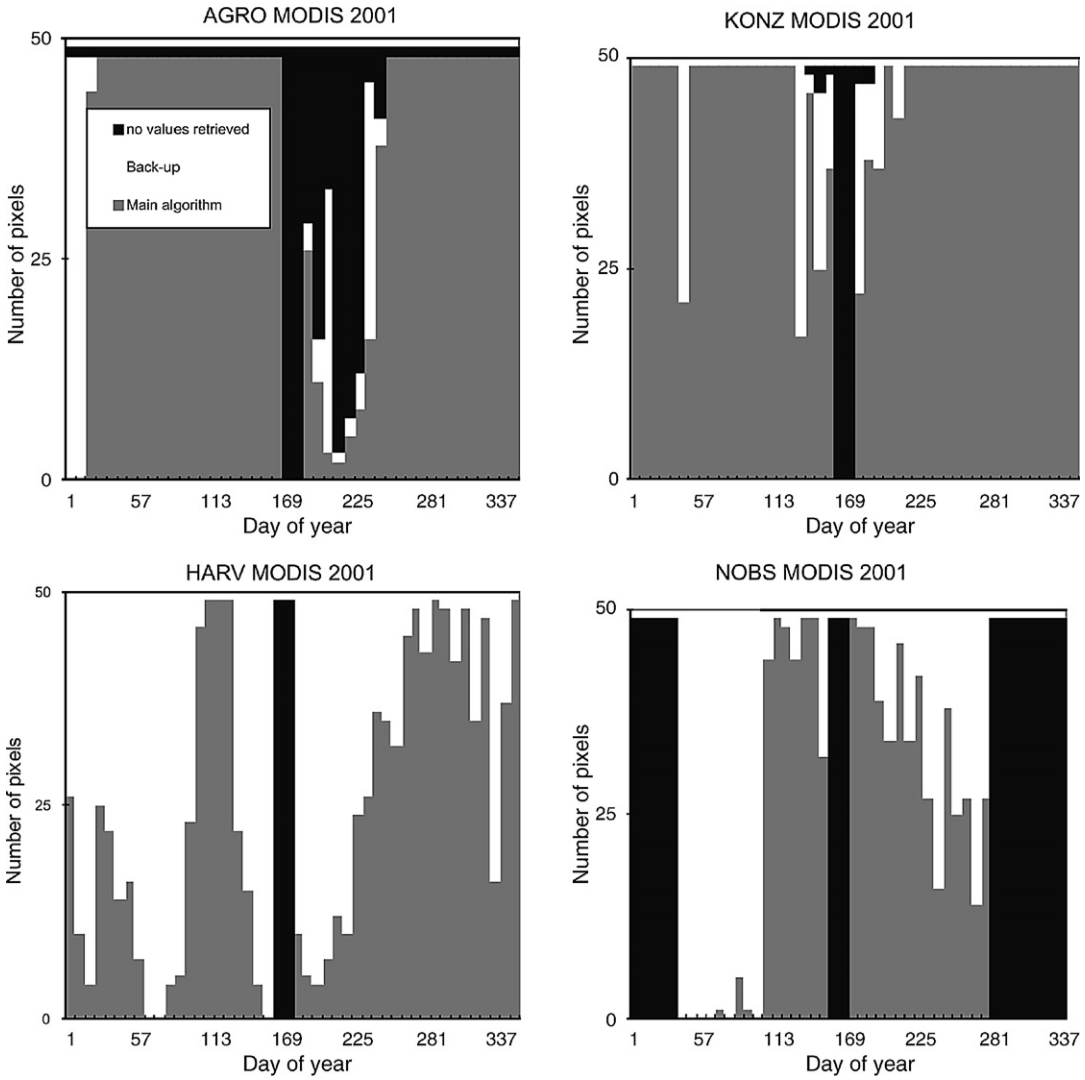

Fig. 6. Relative proportions of pixels with shown origin of calculated LAI value at each site in 2001, as represented in MODIS LAI product.

et al. (2006a) recently reported that in the new prototype Collection 5 product winter LAI already decreases to <0.5 at this location. This is in better agreement with the VGT product. MODIS produces fairly stable values around LAI of 6 during the summer, while the VGT trajectory is more variable due to a series of poorer quality data from the mid-summer. The BigFoot LAI of 4.1 is smaller than the VGT and MODIS values. In the case of MODIS the difference reaches a magnitude of 2. The field measurements were acquired using LICOR-2000 instrument according to the methodology outlined by Gower et al. (1999). However, clumping index values were not obtained for the site and the BigFoot HARV data were not corrected for foliage clumping, i.e. the effect of non-random leaf spatial distribution. The BigFoot data are thus arguably underestimated in comparison with the true LAI values.

The NOBS site is marked by a very simple seasonal cycle with a linear increase in LAI with the peak around July 20 and a subsequent linear decrease (Fig. 3). BigFoot matches relatively closely VGT in terms of LAI with a difference of less than 0.5. The clumping correction was not an issue with BigFoot in this case as the field estimates were established via allometric methods (Cohen et al., 2006a, 2003). MODIS tended to greatly over-estimate LAI especially during the late summer but there was a close agreement between VGT and MODIS during the early summer. It must be acknowledged the modeled seasonal trajectory by the VGT LAI product outside the growing season is spurious for high latitudes. Yang et al. (2006c) and Cohen et al. (2006a) identified poor illumination conditions, extreme solar zenith angles, snow and cloud contamination, and the signal from the understory as the main factors for the similarly poor performance of the MODIS LAI product at high latitudes. The same factors also affect the quality of the VGT LAI product for high latitude estimates during the winter season, but we believe that leaf chlorophyll content may also be an important factor.

BigFoot LAI validation data were also available for 2001 except for the AGRO site. Seasonal trajectories were further produced from MODIS and VGT for 2003. Figs. 4 and 5 show the results. The greatest difference among the various years was observed at AGRO. This was caused by the variation of crops present at the site during different years. NOBS was characterized by the smallest inter-annual differences in the trajectory. In 2001 VGT estimates were also closely matched with BigFoot. MODIS LAI retrievals for NOBS were rather unstable and over-estimated. On the other hand, VGT tended to underestimate LAI for the KONZ site in 2001; both MODIS and VGT estimates were again very similar during 2003. Seasonal trajectories during the main growing season were also reasonably similar for the HARV site in 2001 and 2003. Similar discrepancies were observed between BigFoot and the low resolution products in 2000 and 2001. This further confirms the systematic nature of these underestimated BigFoot data due to an unaccounted clumping effect and its importance in producing reliable validation data (Chen & Cihlar, 1996; Leblanc et al., 2005). MODIS was characterized by a greater standard deviation of the LAI predictions than VGT for every site and year in which the comparisons were made.

The relative instability of MODIS estimates was further examined by comparing the changing proportions of values produced by the main RT and back-up algorithm through the year. The results offer very similar patterns for all three years and only results for 2001 are presented here (Fig. 6). With the exception of NOBS, a significant amount of MODIS retrievals comes from a back-up algorithm during the peak of the growing season (KONZ, HARV) or is not produced at all (AGRO). This is not an optimal situation since most of the validation effort is usually carried out during the summer period. The comparison of site averages, calculated from the main RT values only and then with back-up results included for year 2001, is shown in

Table 4
Comparison of calculated average LAI values over BigFoot sites from MODIS data, using available Quality 0 level estimates only, and averages calculated by using back-up algorithms values as well

Day	AGRO		HARV		KONZ		NOBS	
	Q1	Back-up	Q1	Back-up	Q1	Back-up	Q1	Back-up
1	0.00	0.10	3.13	2.82	0.32	0.32	0.00	0.00
9	0.00	0.10	3.26	1.44	0.32	0.32	0.00	0.00
17	0.23	0.22	2.73	0.81	0.32	0.32	0.00	0.00
25	0.94	0.94	2.60	2.09	0.34	0.34	0.00	0.00
33	0.69	0.69	2.38	2.00	0.30	0.30	0.00	0.00
41	0.84	0.84	1.99	1.05	0.11	0.11	0.00	0.22
49	0.30	0.30	3.29	1.91	0.57	0.57	0.00	0.67
57	0.76	0.76	0.19	0.26	0.79	0.79	0.00	0.29
65	0.35	0.35	0.00	0.69	0.31	0.31	0.00	0.23
73	0.37	0.37	0.00	0.63	0.29	0.29	0.10	0.14
81	0.38	0.38	0.18	0.49	0.33	0.33	0.00	0.21
89	0.45	0.45	0.12	0.51	0.35	0.35	0.12	0.16
97	0.50	0.50	0.75	0.97	0.47	0.47	0.10	0.20
105	0.47	0.47	1.78	1.78	0.55	0.55	0.00	0.20
113	0.52	0.52	2.26	2.26	0.76	0.76	2.49	2.70
121	0.53	0.53	4.79	4.79	1.23	1.23	2.06	2.06
129	0.55	0.55	5.07	5.07	1.54	1.54	2.59	2.62
137	0.52	0.52	6.08	6.04	0.84	1.23	2.12	2.29
145	0.70	0.70	6.49	6.15	2.15	2.18	2.62	2.62
153	1.19	1.19	5.45	5.91	2.30	3.04	3.90	3.90
161	1.16	1.16	0.00	6.10	1.62	2.06	4.44	3.81
185	3.32	3.32	4.79	5.81	1.10	2.62	4.99	4.99
193	2.59	3.09	5.98	6.01	1.85	2.23	5.03	5.04
201	4.33	2.57	4.93	6.01	1.23	1.58	4.34	4.37
209	1.85	2.07	6.60	6.16	1.84	1.84	4.03	4.24
217	2.66	2.91	6.18	6.13	1.80	1.90	3.25	3.87
225	2.65	2.85	5.62	6.00	1.61	1.61	3.67	3.73
233	2.33	2.20	6.53	6.26	1.84	1.84	2.76	3.02
241	2.50	2.57	6.49	6.31	1.74	1.74	3.49	3.70
249	1.33	1.33	6.38	6.30	1.63	1.63	2.64	3.71
257	1.03	1.03	6.00	6.02	1.67	1.67	2.35	3.50
265	0.69	0.69	5.95	5.98	1.44	1.44	1.50	2.31
273	0.61	0.61	5.40	5.45	1.49	1.49	1.78	2.87
281	0.22	0.22	5.13	5.14	1.17	1.17	0.92	1.95
289	0.47	0.47	3.49	3.69	1.01	1.01	0.56	0.53
297	0.42	0.42	2.72	2.72	0.65	0.65	2.01	1.57
305	0.40	0.40	2.66	2.69	0.51	0.51	0.00	0.00
313	0.39	0.39	1.96	2.23	0.48	0.48	0.00	0.00
321	0.63	0.63	2.27	2.31	0.43	0.43	0.00	0.00
329	0.36	0.36	2.08	2.57	0.35	0.35	0.00	0.00
337	0.71	0.71	1.96	2.05	0.37	0.37	0.00	0.00
345	0.49	0.49	1.96	2.74	0.41	0.41	0.00	0.00
353	0.64	0.64	2.26	2.74	0.37	0.37	0.00	0.00
361	0.31	0.31	2.45	2.45	0.35	0.35	0.00	0.00

Table 4. The biggest differences are observed at the HARV site, where the inclusion of back-up values actually resulted in lower LAI averages. The differences were negligible in most of the cases for AGRO and KONZ sites. Differences around LAI of 1 were observed for the NOBS site from day 249 to day 281. However, BigFoot LAI was available for day 195 when both alternatives of MODIS product closely matched.

The findings presented above document that the VGT product seems to deliver reliable information within the snow free growing season about the seasonal cycle of LAI at the four BigFoot sites. The seasonal trajectories matched very closely with MODIS during the start and end of the growing season in most cases except for evergreen conifers. VGT tended to produce good and stable results during the maximum growing period. Both MODIS and VGT LAI values seemed to underestimate LAI at the KONZ site. The standard deviation of VGT LAI during the growing season is smaller than that of MODIS LAI. The use of the LACC smoothing method in the VGT LAI production procedure is considered to be effective in securing a good quality of the product. VGT estimates were also shown to match closely with BigFoot data at three out of four sites.

It is interesting to observe that results from both VGT and MODIS main algorithm approaches tend to deliver mutually corresponding retrievals for grassland and cropland biomes (AGRO, KONZ). The one-dimensional RT model is invoked for these biomes in MODIS approach (Knyazikhin et al., 1998a). Minimal leaf clumping and leaf distribution are very close from that the current MODIS RT methodology originally evolved from (Myneni et al., 1991, 1997), i.e. the canopy is assumed to be a homogeneous medium of infinitesimal scatters (Goel, 1989; Myneni et al., 1989; Pinty & Verstraete, 1998). However, these assumptions do not hold for forest canopies and the full 3-D method is applied for the biomes in both algorithms, although the VGT algorithm is based on a GO model (Four Scale) with a multiple scattering scheme. The largest differences between these two products are observed in forested sites with VGT LAI retrievals being mostly closer to the field LAI estimates than the MODIS retrievals.

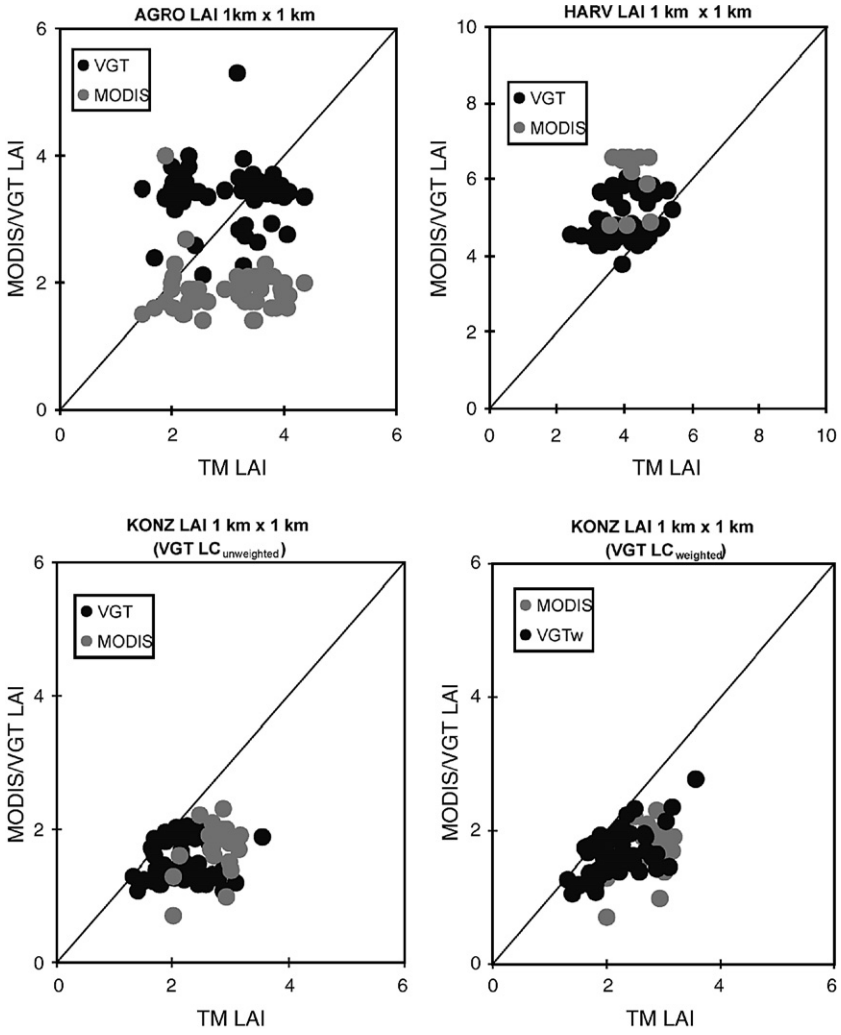

Fig. 7. Comparisons of MODIS (grey) and VGT (black) LAI values for year 2000 with those retrieved from ETM+ map of BigFoot sites. The VGT and MODIS LAI were calculated at 1-km resolution, and the ETM+ LAI was calculated at 25-m resolution. The effect of improving LAI relationship by weighting LAI retrievals land cover fractions within coarse resolution VGT pixels is shown for KONZ site. See text for further details.

We believe the core of the problem lies in the way the radiation interaction with forest canopies with complex structures is modeled. MODIS LUTs of the main algorithm store only a single-scattering albedo at a reference wavelength and at the red and NIR wavelengths (Shabanov et al., 2005), and this single scattering albedo is used to estimate multiple scattering in successive orders in turbid media (Knyazikhin et al., 1998a). The multiple scattering scheme, used for producing the LUTs in the VGT LAI algorithm, addresses the geometrical effects on higher order scattering that can not be accounted for within turbid media-based RT models because the mutual shadowing effects among large geometrical structures (e.g. tree crowns) can not be effectively modeled without explicit mathematical description of these structures. The Four-Scale multiple scattering scheme is based on view factors among sunlit and shaded parts of tree crowns in the canopy, the background and the sky (Chen & Leblanc, 2001). This scheme can thus capture the strong multiple scattering among tree crowns which is the major scattering component in forest canopies, although multiple scattering within tree crowns is still a weakness in this GO model. This scheme is also effective in stimulating the angular dependence of the first, second, and higher order scattering as affected by sun and view angles and the canopy structure and in particular the strong enhancement of reflectance due to multiple scattering around the hotspot — the feature that turbid media RT approaches can not easily simulate with reasonable radiance magnitude and angular width. For the coming MODIS Collection 5 product, a new stochastic RT model has been applied to achieve a better consistency of simulated and MODIS surface reflectances (Shabanov et al., 2005). It remains to be seen if the modification will improve the quality of MODIS retrievals in comparison with ground data.

The quality of the retrievals is also influenced by the length of the compositing period. Shabanov et al. (2005) documented, using a prototype Collection 5 product, that extending the MODIS compositing period from 8 to 10 days reduces the number of back-up LAI values by 15%. This also includes a decrease in the retrieval uncertainties, assuming the phenological changes during the compositing period are not significant.

4.3. BigFoot–MODIS–VGT comparison: pixel-by-pixel

Although pixel-by-pixel comparisons were not attempted in previous MODIS LAI validations (Cohen et al., 2006a, 2003; Tan et al., 2005; Yang et al., 2006a), we believe that a validation is not complete without doing this comparison. Fig. 7 shows four selected scatter-plots for the pixel-by-pixel comparisons of the LAI products. BigFoot estimates were aggregated from 25 m to

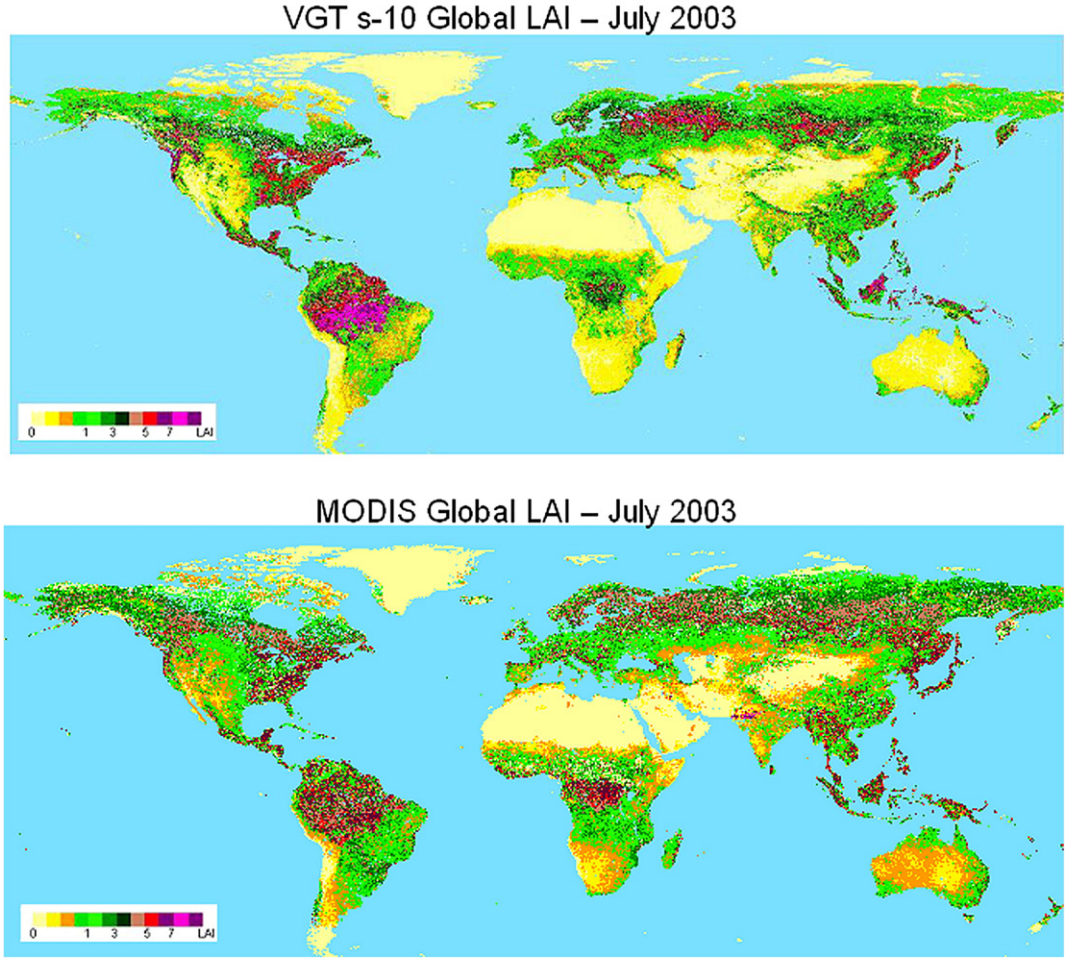

Fig. 8. Color-coded global map of VEGETATION and MODIS LAI fields from the peak of boreal summer — July 2003.

1 km resolution and matched with corresponding low resolution pixels of MODIS and VGT. VGT and MODIS scenes were selected according to their acquisition period to overlap with the dates of BigFoot ETM+ scenes. The scatter-plot for the AGRO site confirms the effectiveness of applying the LACC smoothing method. Both VGT and MODIS original retrievals were poor in quality due to unfavorable atmospheric conditions. The VGT LAI values were generally under-estimated. The main MODIS RT algorithm failed and the back-up filtered values were produced instead. Fig. 7 shows that the LACC method succeeded in reviving the relationship between the final VGT product and BigFoot LAI values as the values are equally occupying the sides of the 1:1 regression line. In contrast, MODIS retrievals bear virtually no relationship with BigFoot data. The median relative absolute error (RAE) for the AGRO site was 88% for the MODIS LAI product, while the RAE of the VGT LAI product was half of this value. The RAE value was 25% for the VGT LAI estimate and 35% for the MODIS LAI estimate at the HARV site. The over-estimation of LAI values by VGT and MODIS in the HARV scatter-plot can be explained by the omission of the clumping effect in the BigFoot retrievals. RAE values for the NOBS site were 37% for the VGT LAI product and 65% for the MODIS LAI product. MODIS LAI estimates had smaller RAE value (47%) than VGT LAI product (76%) at the KONZ site. Fig. 7 further demonstrates the effect of including the contextual information in the input land cover map for the VGT LAI algorithm at the KONZ site. Weighting LAI according to the land cover fractions within each 1 km × 1 km pixel improved the slope of the BigFoot–VGT relationship as it follows a similar vector direction as the 1:1 regression line. The treatments were carried out for other sites as well, but the results did not differ from the original plots due to the homogeneity and limited variation of the land cover within these sites.

The scatter-plots are produced for very small areas (7 km × 7 km). Geolocation uncertainties and pixel-shift errors due to point spread function may not change the general trends in the plotted values of the coarse resolution products and BigFoot data, but they can contribute to the observed scattering of the values in the plots.

4.4. MODIS and VGT global LAI maps

Both global LAI products are displayed in Fig. 8 from the peak period of the boreal summer. Fig. 5 offers an explanation for the difference in LAI values for boreal forests.

At NOBS, MODIS tended to significantly overestimate the LAI values measured by BigFoot or VGT. The similar behavior over boreal forest areas can be observed in Fig. 8. This concurs with the findings of Shabanov et al. (2005) about the anomalies of retrievals over woody vegetation in the Collection 4 data. Shabanov et al. (2005) concluded this behavior at high LAI values in Collection 4 was due to the errors in BRDF modeling for black soil sub-problem of the algorithm.

Smaller LAI differences (LAI diff. < 0.5; Fig. 9) are present over certain areas with herbaceous vegetation. This is linked to the poorer data quality of the MODIS retrievals during winter and summer months. A large number of values are then produced by the back-up algorithm. Tan et al. (2005) showed the back-up algorithm overestimates can amount up to a world-wide difference of LAI = 1.5 against RT-algorithm retrievals during the peak boreal summer. With respect to the VGT performance over the KONZ site in 2003 (Fig. 5), an under-estimation of LAI (LAI diff. < 0.5) by the VGT algorithm within certain types of herbaceous vegetation cannot be excluded as well.

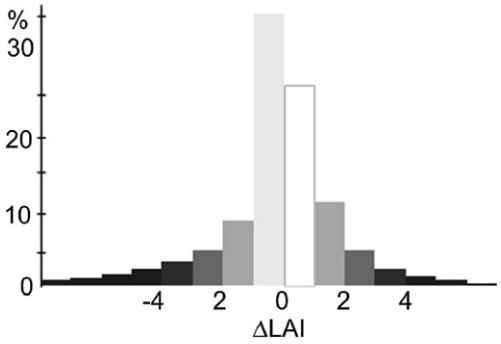

Fig. 9. VGT-MODIS July 2003 global map differences by land surface area. Negative values signify LAI over-estimation by MODIS, positive values mark higher LAI values in VGT LAI product.

5. Conclusions

This research is focused on the validation of a new global LAI product from SPOT4-VGT data. This validation was carried out by means of comparing seasonal LAI trajectories with the MODIS Collection 4 product over four BigFoot sites in 2000, 2001, and 2003. BigFoot ETM+ LAI maps in 2000 and 2001, directly based on field measurements, were used for verification of the retrievals. A reasonable agreement was found between MODIS and VGT seasonal trajectories at the BigFoot sites. This was the case especially at the start and end of the growing season except for the NOBS site. However, they differed during the summer periods. A good agreement between VGT and BigFoot was observed at three out of four sites. MODIS values tended to be unstable with large standard deviations and generally overestimated LAI during the peak of the growing seasons. The median relative absolute errors of the products ranged from 25% (VGT LAI estimate for the HARV site) to 88% (MODIS LAI product for the AGRO site). It was demonstrated that the relatively poor performance of MODIS Collection 4 is caused by the failure of the main radiative-transfer (RT) based algorithm to produce LAI values. Following Tan et al. (2005), we assume this is due to the persisting problems of MODIS Collection 4 to match modeled and measured reflectances from the MODIS sensor. Yang et al. (2006a) reported improved LAI retrievals in the prototype Collection 5 version of the MODIS product, where the amount of over-estimation of the LAI retrievals should be further limited, especially outside the growing season.

At the HARV site, the importance of correcting the field measurements for clumping effects was demonstrated. Since this correction was not done in this BigFoot site, its LAI values were significantly lower than both MODIS and VGT estimates

for this site. The use of the sub-pixel land cover information in retrieving LAI with VGT data considerably improved the quality of LAI estimates for the KONZ site in comparison with a BigFoot ETM+ LAI map. This is in agreement with our validation results for seven selected scenes in Canada (Pisek et al., in press). Similar improvements for the other three BigFoot sites were very small due to their land cover homogeneity.

The results of this study suggest that the new global VGT product could be a sound alternative to the MODIS product, although further validations of both products are still needed in other regions. The validation is needed particularly during the key phenological periods and the in-situ measurement activities in this direction are encouraged. The synergy between the ground measurements at Fluxnet sites (Baldocchi et al., 2001) and the remote sensing validation could also improve the representativeness of sites. As this study recognized the importance of the correct assessment of the foliage clumping effect, future work will be dedicated to the production of global pixel-specific clumping index and forest background reflectance maps that would serve as an input for the VGT LAI algorithms.

Acknowledgements

This study is supported by a Discovery Grant of the Natural Science and Engineering Council of Canada. We greatly appreciate the efforts of Warren Cohen, David Turner, Stith Gower, and Steven Running of the BigFoot project. The authors would like to thank three anonymous reviewers for their helpful constructive comments on the manuscript. Leslie Erin Quinn and Thom Jones helped with English style corrections.

References

Abuelgasim, R. A., Fernandes, R. A., & Leblanc, S. G. (2006). Evaluation of national and global LAI products derived from optical remote sensing instruments over Canada. *Institute of Electrical and Electronics Engineers (IEEE) Transactions on Geoscience and Remote Sensing*, *44*(7), 1872−1884.

Baldocchi, D., Falge, E., Gu, L., Olson, R., Hollinger, D., Running, S., et al. (2001). FLUXNET: A new tool to study the temporal and spatial variability of ecosystem-scale carbon dioxide, water vapor and energy flux densities. *Bulletin of the American Meteorological Society*, *82*, 2415−2434.

Band, L. E., Peterson, D. L., Running, S. W., Dungan, J., Lathrop, R., Coughlan, J., et al. (1991). Forest ecosystem processes at the watershed scale: Basis for distributed simulation. *Ecological Modelling*, *56*, 171−196.

Bartholomé, E., & Belward, A. S. (2005). GLC2000: a new approach to global land cover mapping from Earth Observation data. *International Journal of Remote Sensing*, *26*, 1959−1977.

Bonan, G. B. (1995). Land-atmospheric interactions for climate system models: coupling biophysical, biogeochemical and ecosystem dynamical processes. *Remote Sensing of Environment*, *51*, 57−73.

Brown, L., Chen, J. M., Leblanc, S. G., & Cihlar, J. (2000). A shortwave infrared modification to the simple ratio for LAI retrieval in boreal forests: An image and model analysis. *Remote Sensing of Environment*, *71*, 16−25.

Buermann, W., Wang, Y., Dong, J., Zhou, L., Zeng, X., Dickenson, R. E., et al. (2002). Analysis of multiyear global vegetation index data set. *Journal of Geophysical Research*, *107*(D22), 4646.

Campbell, J. L., Burrows, S., Gower, S. T., & Cohen, W. B. (1999). Big-Foot: Characterizing land cover, LAI, and NPP at the landscape scale for EOS/MODIS validation. *Field manual 2.1Environmental Science Division Pub.*, *Vol. 4937* (pp.) Oak Ridge, TN: Oak Ridge National Laboratory.

Chen, J. M. (1996). Canopy architecture and remote sensing of the fraction of photosynthetically active radiation absorbed by boreal conifer forest. *IEEE Transactions on Geoscience and Remote Sensing*, *34*, 1353−1368.

Chen, J. M. (1999). Spatial scaling of a remote sensed surface parameter by contexture. *Remote Sensing of Environment*, *69*, 30−42.

Chen, J. M., & Black, T. A. (1992). Defining leaf-area index for non-flat leaves. *Plant, Cell and Environment*, *15*, 421−429.

Chen, J. M., & Cihlar, J. (1996). Retrieving leaf area index for boreal conifer forests using Landsat TM images. *Remote Sensing of Environment*, *55*, 153−162.

Chen, J. M., & Cihlar, J. (1997). A hotspot function in a simple bidirectional reflectance model for satellite applications. *Journal of Geophysical Research*, *102*, 25907−25913.

Chen, J. M., Deng, F., & Chen, M. (2006). Locally adjusted cubic-spline capping for reconstructing seasonal trajectories of a satellite-derived surface parameter. *IEEE Transactions on Geoscience and Remote Sensing*, *44*, 2230−2238.

Chen, J. M., & Leblanc, S. G. (1997). A 4-scale bidirectional reflection model based on canopy architecture. *IEEE Transactions on Geoscience and Remote Sensing*, *35*, 1316−1337.

Chen, J. M., & Leblanc, S. G. (2001). Multiple-scattering scheme useful for hyperspectral geometrical optical modelling. *IEEE Transactions on Geoscience and Remote Sensing*, *39*, 1061−1071.

Chen, J. M., Menges, C. H., & Leblanc, S. G. (2005). Global derivation of the vegetation clumping index from multi-angular satellite data. *Remote Sensing of Environment*, *97*, 447−457.

Chen, J. M., Pavlic, G., Brown, L., Cihlar, J., Leblanc, S. G., White, H. P., et al. (2002). Validation of Canada-wide leaf area index maps using ground measurements and high and moderate resolution satellite imagery. *Remote Sensing of Environment*, *80*, 165−184.

Chen, J. M., Rich, P. M., Gower, T. S., Norman, J. M., & Plummer, S. (1997). Leaf area index of boreal forests: Theory, techniques and measurements. *Journal of Geophysical Research*, *102*, 29429−29444.

Cihlar, J., Chen, J. M., & Li, Z. (1997). Seasonal AVHRR composite multichannel data sets for scaling up. *Journal of Geophysical Research*, *102*, 29,625−29,640.

Cihlar, J., Latifovic, R., Beaubien, J., Guindon, B., & Palmer, M. (2003). Thematic mapper (TM) based accuracy assessment of a land cover product for Canada derived from SPOT VEGETATION (VGT) data. *Canadian Journal of Remote Sensing*, *29*, 154−170.

Cohen, W. B., Maiersperger, T. K., Turner, D. P., Ritts, W. D., Pflugmacher, D., Kennedy, R. E., et al. (2006a). MODIS land cover and LAI Collection 4 product quality across nine sites in the Western Hemisphere. *IEEE Transactions on Geoscience and Remote Sensing*, *44*, 1843−1857.

Cohen, W.B., Maiersperger, T.K., & Pflugmacher, D. (2006b). *BigFoot Land Cover Surfaces for North and South American Sites, 2000–2003. Data set*. Available on-line [http://www.daac.ornl.gov] from Oak Ridge National Laboratory Distributed Active Archive Center, Oak Ridge, Tennessee, U.S.A.

Cohen, W. B., Maiersperger, T. K., Yang, Z., Gower, S. T., Turner, D. P., Ritts, M., et al. (2003). Comparisons of land cover and LAI estimates derived from ETM+ and MODIS for four sites in North America: A quality assessment of 2000/2001 provisional MODIS products. *Remote Sensing of Environment*, *88*, 233−255.

Coops, N. C., Waring, R. H., & Landsberg, J. J. (2001). Estimation of potential forest productivity across the Oregon transect using satellite data and monthly weather records. *International Journal of Remote Sensing*, *22*, 3797−3812.

Cracknell, A. P. (1998). Synergy in remote sensing — what's in a pixel? *International Journal of Remote Sensing*, *19*, 2025−2047.

Deng, D., Chen, J. M., Plummer, S., Chen, M., & Pisek, J. (2006). Global LAI algorithm integrating the bidirectional information. *IEEE Transactions on Geoscience and Remote Sensing*, *44*, 2219−2229.

Dickinson, R. E. (1995). Land-atmosphere interaction. *Review of Geophysics*, *33*, 917−922. Supplement.

Fensholt, R., Sandholt, I., & Rasmussen, M. S. (2004). Evaluation of MODIS LAI, fAPAR and the relation between fAPAR and NDVI in a semi-arid

environment using in situ measurements. *Remote Sensing of Environment*, *91*, 490−507.

Fernandes, R., Butson, C., Leblanc, S., & Latifovic, R. (2003). Landsat-5 TM and Landsat-7 ETM+ based accuracy assessment of leaf area index products for Canada derived from SPOT-4 VEGETATION data. *Canadian Journal of Remote Sensing*, *29*, 241−258.

Frank, A. B. (2002). Carbon dioxide fluxes over a grazed prairie and seeded pasture in the Northern Great Plains. *Environmental Pollution*, *116*, 397−403.

Goel, N. (1989). Inversion of canopy reflectance models for estimation of biophysical parameters from reflectance data. In G. Asrar (Ed.), *Theory and Applications of Optical Remote Sensing* (pp. 205−250). New York: Wiley Interscience.

Gower, S., Kucharik, C., & Norman, J. (1999). Direct and indirect estimation of leaf area index, fAPAR, and net primary production of terrestrial ecosystems. *Remote Sensing of Environment*, *70*, 29−51.

Hall, F. G., Huemmrich, F., & Goward, S. N. (1990). Use of narrow-band spectra to estimate the fraction of absorbed photosynthetic active radiation. *Remote Sensing of Environment*, *32*, 47−54.

Harding, D. J., Lefsky, M. A., Parker, G. G., & Blair, J. B. (2001). Laser altimeter canopy height profiles — methods and validation for closed-canopy, broadleaf forests. *Remote Sensing of Environment*, *76*, 283−297.

Huemmrich, K. F., Privette, J. L., Mukelabai, M., Myneni, R. B., & Knyazikhin, Y. (2005). Time-series validation of MODIS land biophysical products in a Kalahari Woodland, Africa. *International Journal of Remote Sensing*, *26*, 4381−4398.

Kimball, J., Running, S. W., & Nemani, R. (1997). An improved method for estimating surface humidity from daily minimum temperature. *Agricultural and Forest Meteorology*, *85*(1−2), 87−98.

Knyazikhin, Y., Martonchik, J. V., Myneni, R. B., Diner, D. J., & Running, S. W. (1998a). Synergistic algorithm for estimating vegetation canopy leaf area index and fraction of absorbed photosynthetically active radiation from MODIS and MISR data. *Journal of Geophysical Research*, *103*, 32257−32274.

Knyazikhin, Y., Martonchik, J. V., Diner, D. J., Myneni, R. B., Vertraete, M., Pinty, B., et al. (1998b). Estimation of vegetation canopy leaf area index and fration of absorbed photosynthetically active radiation from atmosphere-corrected MISR data. *Journal of Geophysical Research*, *103*, 32239−32356.

Lacaze, R., Chen, J. M., Roujean, J. -L., & Leblanc, S. G. (2002). Retrieval of vegetation clumping index using hot spot signatures measured by POLDER instrument. *Remote Sensing of Environment*, *79*, 84−95.

Leblanc, S., Chen, J. M., Fernandes, R., Deering, D. W., & Conley, A. (2005). Methodology comparison for canopy structure parameters extraction from digital hemispherical photography in boreal forests. *Agricultural and Forest Meteorology*, *129*, 187−207.

Liu, J., Chen, J. M., Cihlar, J., & Park, W. (1997). A process-based boreal ecosystems productivity simulator using remote sensing inputs. *Remote Sensing of Environment*, *62*, 158−175.

Loveland, T. R., Zhu, Z., Ohlen, D. O., Brown, J. F., Redd, B. C., & Yang, L. (2000). An analysis of the IGBP global land cover characterization process. *Photogrammetric Engineering and Remote Sensing*, *65*, 1021−1031.

Magill, A. H., Aber, J. D., Currie, W. S., Nadelhoffer, K. J., Martin, M. E., McDowell, W. H., et al. (2004). Ecosystem response to 15 years of chronic nitrogen additions at the Harvard Forest LTER, Massachusetts, USA. *Forest Ecology and Management*, *196*, 7−28.

Morisette, J. T., Baret, F., Privette, J., Myneni, R. B., Nickeson, J., Garrigues, S., et al. (2006). Validation of global moderate resolution LAI Products: a framework proposed within the CEOS Land Product Validation sub-group. *IEEE Transactions on Geoscience and Remote Sensing*, *44*(1), 1801−1817.

Myneni, R. B., Hall, F. G., Sellers, P. J., & Marshak, A. L. (1995). The interpretation of spectral vegetation indexes. *IEEE Transactions on Geoscience and Remote Sensing*, *33*, 481−486.

Myneni, R. B., Knyazikhin, Y., Privette, J. L., Glassy, J., Tian, Y., Wang, Y., et al. (2002). Global products of vegetation leaf area and fraction absorbed PAR from year one of MODIS data. *Remote Sensing of Environment*, *83*, 214−231.

Myneni, R. B., Marshak, A. L., & Knyazikhin, Y. (1991). Transport theory for leaf canopies with finite dimensional scattering centers. *Journal of Quantitative Spectroscopy & Radiative Transfer*, *46*, 259−280.

Myneni, R. B., Nemani, R. R., & Running, S. W. (1997). Estimation of global leaf area index and absorbed par using radiative transfer models. *IEEE Transactions on Geoscience and Remote Sensing*, *35*, 1380−1393.

Myneni, R. B., Ross, J., & Asrar, G. (1989). A review on the theory of photon transport in leaf canopies in slab geometry. *Agricultural and Forest Meteorology*, *45*, 1−153.

Nouvellon, Y., Rambal, S., Lo Seen, D., Moran, M. S., Lhomme, J. P., Bégué, A., et al. (2000). Modelling of daily fluxes of water and carbon from shortgrass steppes. *Agricultural and Forest Meteorology*, *100*, 137−153.

Oleson, K. W., Sarlin, S., Garrison, J., Smith, S., Privette, J. L., & Emery, W. (1995). Unmixing multiple land-cover type reflectances from coarse spatial resolution satellite data. *Remote Sensing of Environment*, *54*, 98−112.

Pinty, B., & Verstraete, M. M. (1998). Modeling the scattering of light by homogeneous vegetation in optical remote sensing. *Journal of Atmospheric Science*, *55*, 137−150.

Pisek, J., Chen, J. M., & Deng, F. (in press). Assessment of a new global leaf area index dataset from SPOT-4 VEGETATION data over selected sites in Canada. *Canadian Journal of Remote Sensing*.

Puyou-Lascassies, P., Flouzat, G., Gay, M., & Vignolles, C. (1994). Validation of the use of multiple linear regression as a tool for unmixing coarse spatial resolution images. *Remote Sensing of Environment*, *49*, 155−166.

Rahman, H., & Dedieu, G. (1994). SMAC: a simplified method for the atmospheric corrections of satellite measurements in the solar spectrum. *International Journal of Remote Sensing*, *15*, 123−143.

Roujean, J. L., Leroy, M., & Deschamps, P. Y. (1992). A bidirectional reflectance model of the earth's surface for the correction of remote sensing data. *Journal of Geophysical Research*, *97*, 20455−20468.

Running, S. W., Collatz, G. J., Washburne, J., Sorooshian, S., Dunne, T., Dickinson, R. E., et al. (1999). Land ecosystems and hydrology. In M. D. King (Ed.), *EOS science plan* (pp. 197−259). Greenbelt: National Aeronautics and Space Administration.

Schaaf, C., Strahler, A., Lucht, W., Tsang, T., Gao, F., Li, X., et al. (2002). The At launch MODIS BRDF and Albedo Science Data Product. *Remote Sensing of Environment*, *83*, 135−148.

Sellers, P. J., Hall, F. G., Kelley, R. D., Black, A., Baldocchi, D., Berry, J., et al. (1997). BOREAS in 1997: Experiment overview, scientific results, and future directions. *Journal of Geophysical Research*, *102*(D24), 28731−28769.

Sellers, P. J., Los, S. O., Tucker, C. J., Justice, C. O., Dazlich, D. A., Collatz, C. J., et al. (1994). A 1 x 1 NDVI data set for global climate studies. Part 2: The generation of global fields of terrestrial biophysical parameters from the NDVI. *International Journal of Remote Sensing*, *15*, 3519−3545.

Shabanov, N. V., Huang, D., Yang, W., Tan, B., Knyazikhin, Y., Myneni, R. B., et al. (2005). Optimization of the MODIS LAI and FPAR algorithm performance over broadleaf forests. *IEEE Transactions on Geoscience and Remote Sensing*, *43*, 1855−1865.

Su, Z. (2000). Remote sensing of land use and vegetation for mesoscale hydrological studies. *International Journal of Remote Sensing*, *21*, 213−233.

Tan, B., Hu, J., Huang, D., Yang, W., Zhang, P., Shabanov, N. V., et al. (2005). Assessment of the broadleaf crops leaf area index product from the terra MODIS Instrument. *Agricultural and Forest Meteorology*, *135*, 124−134.

Wang, Y., Woodcock, C. E., Buermann, W., Stenberg, P., Voipio, P., Smolander, H., et al. (2004). Evaluation of the MODIS LAI algorithm at a coniferous forest site in Finland. *Remote Sensing of Environment*, *91*, 114−127.

Weiss, M., Baret, F., Myneni, R. B., Pragnere, A., & Knyazikhin, Y. (2000). Investigation of a model inversion technique for the estimation of crop characteristics from spectral and directional reflectance data. *Agronomie*, *20*, 3−22.

Yang, W., Huang, D., Tan, B., Stroeve, J. C., Shabanov, N. V., Knyazikhin, Y., et al. (2006). Analysis of leaf area index and fraction of PAR absorbed by vegetation products from the Terra MODIS Sensor: 2000–2005. *IEEE Transactions on Geoscience and Remote Sensing*, *44*, 1829−1842.

Yang, W., Shabanov, N. V., Huang, D., Wang, W., Dickinson, R. E., Nemani, R. R., et al. (2006). Analysis of leaf area index products from combination of MODIS Terra and Aqua data. *Remote Sensing of Environment*, *104*, 297−312.

Yang, W., Tan, B., Huang, D., Rautiainen, M., Shabanov, N. V., Wang, Y., et al. (2006). MODIS leaf area index products: From validation to algorithm improvement. *IEEE Transactions on Geoscience and Remote Sensing*, *44*, 1885−1898.